Throughput Enhancement Through Dynamic Fragmentation in Wireless LANs

Byung-Seo Kim, *Student Member, IEEE*, Yuguang Fang, *Senior Member, IEEE*, Tan F. Wong, *Senior Member, IEEE*, and Younggoo Kwon

***Abstract*—Many rate-adaptive MAC protocols have been proposed in the past for wireless local area networks (LANs) to enhance the throughput based on channel information. Most of these protocols are receiver based and employ the RTS/CTS collision avoidance handshake specified in the IEEE 802.11 standard. However, these protocols have not considered the possibility of bursty transmission of fragments in the corresponding rate adaptation schemes. In this article, a rate-adaptive protocol with dynamic fragmentation is proposed to enhance the throughput based on fragment transmission bursts and channel information. Instead of using one fragmentation threshold in the IEEE 802.11 standard, we propose to use multiple thresholds for different data rates so more data can be transmitted at higher data rates when the channel is good. In our proposed scheme, whenever the rate for the next transmission is chosen based on the channel information from the previous fragment transmission, a new fragment is then generated using the fragment threshold for the new rate. In this way, the channel condition can be more effectively used to squeeze more bits into the medium. We evaluate this scheme under a time-correlated fading channel model and show that the proposed scheme achieves much higher throughput than other rate-adaptive protocols.**

***Index Terms*—Fragmentation, MAC, rate-adaptive MAC protocol, wireless local area network (LAN).**

I. Introduction

A TYPICAL wireless communication link in a wireless local area network (LAN) is time varying. It is challenging to more effectively design transmission schemes based on the channel condition. Many adaptive transmission schemes to enhance the throughput performance have been proposed in the literature. Many of these schemes vary the data rate, transmission power, and packet length. One of the popular schemes is based on rate adaptation. This scheme includes an adaptive transmission method that employs different modulation and coding schemes to adjust the data rate based on the channel condition in terms of the signal-to-noise ratio (SNR). The basic idea is to employ a higher-level modulation scheme when a higher SNR is detected as long as the target error rate is satisfied. The target error rate can be characterized by the bit error rate (BER), symbol error rate (SER), or packet error rate (PER), specified by a designer. For the receiver-based rate adaptation schemes, the receiver usually carries out the channel estimation and rate selection, and the selected rate is then fed back to the transmitter.

Many rate adaptation schemes for 2.5G and 3G wireless cellular networks using centralized TDMA-based MAC protocols have been proposed in [1]–[7]. In addition, the power control schemes considering power saving and rate adaptation have been proposed in [6] and [7]. All these schemes work at the base station in a centralized fashion. However, to our best knowledge, only a few MAC protocols with rate adaptation have been proposed for distributed wireless LANs. In [9], the auto rate fallback (ARF) protocol is proposed. In ARF, the sender selects the rate based on the packet transmission failure rate. Whenever transmission failures occur, a lower rate will be chosen. The performance of this scheme with threshold selection for fallback is evaluated in [10]. In [18], a similar scheme is also designed based on the time-out of the acknowledgment (ACK) frame. In [11] and [12], the authors use the RTS/CTS collision avoidance handshaking to exchange channel information and then select the rate accordingly. Specifically, in the receiver-based auto rate (RBAR) MAC protocol proposed in [11], channel estimation and rate selection are carried out by the receiver based on the RTS transmission, and the selected rate is sent back to the sender in the MAC header of the CTS packet. To enhance transmission reliability of the MAC header, a cyclic redundancy check (CRC) code is added to the MAC header in RBAR. A two-step scheme is proposed to update the network allocation vector (NAV), which is a critical component in the virtual carrier sensing in IEEE 802.11 MAC. More details about this scheme are given in Section II. It has been shown that RBAR achieves better throughput performance than ARF because rate adaptation based on channel estimation can better cope with the time-varying nature of the channel than ARF does.

With ARF and RBAR, the sizes of transmitted packets vary and hence all nodes may have different channel access times. This may aggravate the unfairness issue in time. Therefore, in the opportunistic auto rate (OAR) protocol proposed in [13], the authors suggest to allow a sender to use a high data rate to transmit more packets for the duration in which the sender has acquired the channel access right.

In the IEEE 802.11 standard, when a MAC service data unit (MSDU) generated by the logical link control (LLC) layer is larger than the fragmentation threshold, the MSDU is fragmented into smaller-size MAC protocol data units (MPDUs).

Manuscript received July 19, 2003; revised September 15, 2004. This work was supported in part by the U.S. Office of Naval Research under Young Investigator Award N000140210464 and under grant N000140210554, and by the National Science Foundation under Faculty Early Career Development Award ANI-0093241 and under grant ANI-0220287. The review of this paper was coordinated by Dr. O. Ugweje.

B.-S. Kim is with Motorola Inc., Schaumburg, IL 60196 USA (e-mail: Byungseo.kim@motorola.com).

Y. Fang and T. F. Wong are with the Department of Electrical and Computer Engineering, University of Florida, Gainesville, FL 32611 USA (e-mail: fang@ece.ufl.edu; twong@ece.ufl.edu).

Y. Kwon is with the Department of Computer Engineering, Sejong University, Seoul, Korea (e-mail: ygkwon@sejong.ac.kr).

Digital Object Identifier 10.1109/TVT.2005.851361

For many applications, the size of MSDU is often so large that fragmentation is indeed necessary. In [18], a frame prediction scheme is proposed. This scheme predicts the optimal frame size for the next transmission according to the BER under the expected channel quality. However, fragmentation and rate adaptation are not considered in that paper. In [15] and [16], the authors develop a scheme to choose the optimal fragment size based on channel information, such as the achievable data rate and goodput. Therein, although each MSDU can be fragmented according to the channel information, the size of MPDUs remains unchanged during the MSDU transmission, and the transmission scheme is still static in nature although certain optimization is performed. Moreover, in the schemes proposed in [14]–[16], the mechanism for exchanging the channel information is not clearly elaborated. Other fragmentation schemes without rate adaptation are proposed in [17]–[19]. The fragmentation threshold is halved for each transmission failure during the transmission bursts in [17], whereas in [18], it is doubled for each successful transmission and halved for each transmission failure. In [19], the fragmentation size is tuned to allow a fragment to fit in a dwell time in the frequency hopping communication system.

In this article, we propose a new receiver-based MAC protocol based on dynamic fragmentation. The proposed protocol is similar to RBAR and OAR. However, instead of allowing the transmission of multiple packets with a high data rate, we allow a larger MPDU size to reduce the overhead caused by the transmission of multiple fragments when the channel condition is good. In addition, we adapt the fragment size during the MSDU transmission period based on channel condition information obtained from preceding fragment transmission. In addition, a fragment is generated on the fly from the remaining MSDU only when a fragment is ready for transmission, in contrast with the one-time fragmentation for MSDU used in other protocols (e.g., IEEE 802.11 MAC). The rest of this article is organized as follows. Section II reviews the MAC protocol and fragmentation process of IEEE 802.11 MAC and some known rate adaptation schemes pertinent to this article. The proposed scheme is presented in Section III. Section IV describes the simulation environment under which the performance of the proposed scheme is evaluated. In Section V, we provide the conclusions.

II. Background

A. Overview

The DCF mode in IEEE 802.11 MAC is called carrier sense multiple access/collision avoidance (CSMA/CA), which is widely used in wireless LANs. In CSMA/CA, a node having a frame to transmit senses the channel for a distributed inter-frame space (DIFS) idle time to check whether the channel is idle. If the channel is busy, the node defers the transmission until the channel is idle. When the channel is idle during a DIFS idle time, the node chooses its random backoff time and continues to sense the channel during the chosen time period. The backoff timer decrements the chosen time as time goes on. If the channel remains idle when the backoff timer reaches zero, the node sends an RTS frame and the intended receiving node sends a CTS frame back to the sender after a short inter-frame space (SIFS) idle time. Because the RTS and CTS frames contain information about the duration of the incoming data transmission, other nodes overhearing the RTS or CTS packet defer their transmissions for the duration defined by the network allocation vector (NAV). This is the known virtual carrier sensing, which prevents collision during data transmission. After receiving the CTS, the sender transmits a data fragment and the receiver sends an ACK back to the sender after a SIFS idle time. The timing of the protocol used in DCF consists of cycles starting from the DIFS idle period and ending with the ACK.

B. Fragmentation in IEEE 802.11

Fragmentation is the process of dividing a long frame into short frames. Fig. 1 illustrates the fragmentation process in IEEE 802.11 MAC [8]. When an MSDU is passed down from the LLC layer, if the size of the MSDU is greater than the fragmentation threshold *aFragmentationThreshold*, it is divided into smaller fragments. Each fragment, namely an MPDU, becomes a MAC layer frame with a MAC header. Then, a physical layer convergence protocol (PLCP) header and a preamble are added to the MPDU. The resulting frame is called a PLCP protocol data unit (PPDU), which is the frame transmitted by the physical layer over the air. Fragmentation can be used to improve the transmission reliability in hostile wireless environments because the probability of successful transmission increases as the size of MPDU decreases. Usually, in IEEE 802.11 wireless LANs, an MSDU is fragmented into equal-size MPDUs, except for the last one before the transmission attempt. These MPDUs are put into the buffer at the transceiver, and none of them will be refragmented further. All fragments are sent independently, each of which is separately acknowledged. Once a sender contends for and seizes the medium, it will continue to send fragments with SIFS-size gaps between the ACK reception and the start of the subsequent fragment transmission until either all the fragments of the MSDU have been sent or an ACK is not received. When the transmission of a fragment fails, the contention process begins after a DIFS idle time period. The remaining fragments are transmitted when the node seizes the channel again through the contention process. The transmission process for the fragments of an MSDU is called a fragment burst. Because the header of each MAC frame contains the information that defines the duration of the next transmission, the nodes that overhear the header update the NAV value for the next fragment transmission.

C. Proposed Rate-Adaptive Protocols for IEEE 802.11 MAC DCF Mode

The MAC protocols proposed in [11]–[13] use the RTS/CTS frames to exchange the selected data rate during the data transmission period. The receiver uses RTS to carry out channel estimation and rate selection. The selected rate is then fed back to the sender via CTS. The RTS and CTS packets are exchanged at the base rate to ensure all nodes in the radio range can receive them without error. The performance evaluation of these protocols only considers the case when the MSDU size

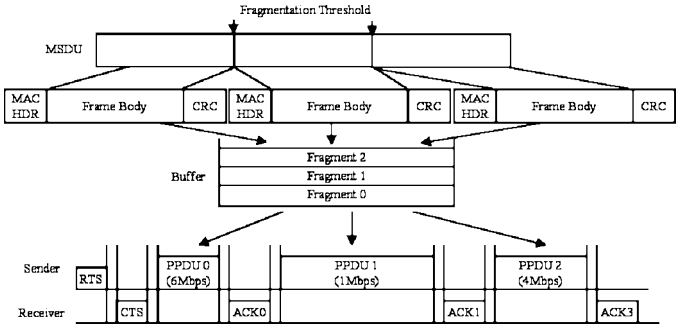

Fig. 1. Conventional fragmentation process and timeline of data transmission with rate adaptation.

is less than *aFragmentationThreshold* (i.e., each node has only one fragment to send in its respective fragment burst). Because all MPDUs are of the same size when using the fragmentation scheme as described previously, the size of a data PPDU varies according to the selected rate so the duration of data transmission varies as shown in Fig. 1. Therefore, because of the variable duration of the data transmission, the duration value in the RTS frame is not the same as the actual transmission duration of the data frame. This causes a NAV update problem for nodes overhearing the RTS and MPDUs. Thus, a two-step process is proposed in the RBAR protocol for NAV update. When the nodes overhearing the CTS packet update the NAV value with the duration calculated from the selected rate, the other nodes overhearing the RTS packet update the NAV value with a tentative duration, which is the duration for transmitting the MPDU at the lowest rate. When the nodes overhearing the RTS packet hear the MPDU, the NAV value is updated to the duration calculated from the rate in the PLCP header of the MPDU.

III. Proposed Protocol

A. Fragmentation Scheme

In this article, we propose a new dynamic fragmentation scheme to enhance throughput under time-varying wireless environment. The proposed scheme contains the following key changes comparing to IEEE802.11 MAC:

- The transmission durations of all fragments, except the last fragment, in the physical layer are set to be the same regardless of the data rate;
- Different *aFragmentationThreshold*s for different rates are used based on the channel condition (i.e., a rate-based fragmentation thresholding [RFT] scheme is employed);
- A new fragment is generated from the fragmentation process only when the rate is decided for the next fragment transmission, resulting in dynamic fragmentation (DF).

In IEEE 802.11, with a single *aFragmentationThreshold*, the sizes of fragments are equal regardless of the channel condition. Therefore, the channel access time for a fragment varies with respect to the selected physical layer data rate. It is generally assumed that the channel remains unchanged during the transmission of a fragment at the base rate. Thus, more data frames can in fact be transmitted when a higher rate is used in the same duration provided that the SNR is high enough to support the higher rate. Due to this observation, the OAR protocol in [13] proposes a multipacket transmission scheme. However, multipacket transmission has a higher overhead because of the additional MAC headers, PHY headers, preambles in data and ACK, and SIFS idle times. To overcome the shortcoming of multipacket transmission, we fix the time duration of all data transmission except for the last fragment. To better understand the mechanism, we show the protocol timelines for the RBAR scheme and our dynamic fragmentation scheme in Fig. 2. To generate fragments with the same time duration in a physical layer, the number of bits in a fragment should be varied based on the selected rate. Thus, it is necessary to have different *aFragmentationThreshold*s for different data rates. When the sender receives the selected rate from the receiver, the next fragment is then generated from the fragmentation process according to the *aFragmentationThreshold* for that rate. Thus, the fragmentation threshold at rate R is

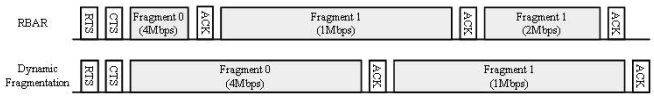

Fig. 2. Timelines for RBAR and the proposed dynamic fragmentation scheme.

$$\mathrm{Threshold}_R = \mathrm{Threshold}_B \cdot \frac{R}{B} \tag{1}$$

where $\mathrm{Threshold}_B$ is the *aFragmentationThreshold* at the base rate B and its unit is bit. At rate R, to transmit the same amount of information contained in an MPDU in the dynamic fragmentation scheme, the additional overhead in the single *aFragmentationThreshold* $(\mathrm{Threshold}_B)$ scheme is

$$\mathrm{Overhead} = (T_{\mathrm{pre}} + T_{\mathrm{PHY\_hdr}} + T_{\mathrm{MAC\_hdr}} + 2 \cdot T_{\mathrm{SIFS}} + T_{\mathrm{ACK}}) \cdot \left(\left\lceil \frac{R}{B} \right\rceil - 1 \right) \tag{2}$$

where $T_{\mathrm{pre}}, T_{\mathrm{PHY\_hdr}}, T_{\mathrm{MAC\_hdr}}$, and T_{ACK} are time durations of the preamble, PHY header, MAC header, and ACK frame; and T_{SIFS} is the SIFS idle time. In (2), $\lceil R/B \rceil$ indicates the number of data MPDUs that are needed in the single *aFragmentationThreshold* scheme to transmit the same amount of data as one MPDU in our fragmentation scheme. From (2), we observe that higher data rate requires larger overhead.

In the fragmentation process in IEEE 802.11 MAC, an MSDU is fragmented into equal-size fragments, which remain unchanged until all fragments in the burst are transmitted. If the channel quality is constant during the transmission of the fragment burst, the target PER can be met. However, this is not guaranteed in a wireless LAN because of two reasons. The first reason is that different fragments of the burst experience different levels of channel quality because of the time-varying nature of the wireless channel. The second reason is that after the transmission of a fragment fails, the sender contends for the channel again to transmit remaining fragments; thus, the channel quality is not guaranteed to be the same as that at the time when the previous fragment is transmitted. To achieve the target PER, both

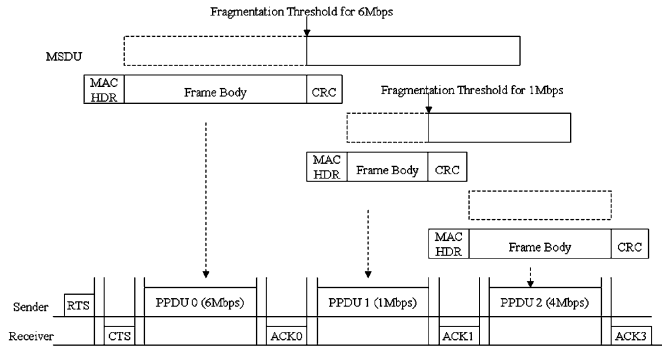

Fig. 3. Dynamic fragmentation process and timeline of data transmission.

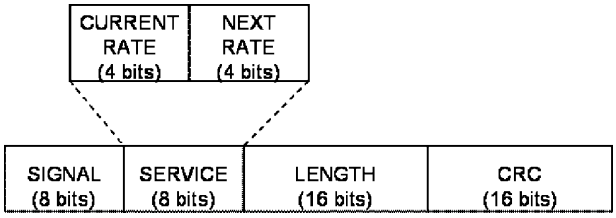

Fig. 4. Physical layer header format in the proposed protocol.

the data rate and a fragment size should vary according to the changing channel condition. Moreover, to better match the varying channel condition, instead of generating all fragments before transmitting the first fragment, each fragment should be generated at the time when the rate is chosen for the next transmission. As a result, the fragments in a burst may not be of the same size. Fig. 3 illustrates the proposed dynamic fragmentation scheme. When the transmission of a fragment fails, the size of the retransmitted fragment may not be the same as that of the originally transmitted fragment because the channel condition may have changed. When the fragment number of the most recently received fragment is the same as that of the already received fragment, the receiver discards the old fragment. Hence, the MSDU size is reduced only when a fragment is transmitted successfully (i.e., the sender receives the ACK from the receiver).

B. Rate-Adaptive MAC Protocol for Fragment Burst

With fragment burst transmission and rate adaptation for each fragment, data and ACK frames also participate in the rate adaptation process in the same way as do the RTS/CTS frames. To support the rate adaptation process of a fragment burst, the physical layer header is modified as shown in Fig. 4. The *service* field in the PLCP header is divided into two 4-bit subfields, namely the current rate and next rate subfields. The *current rate* subfield indicates the data rate of the current frame, whereas the *next rate* subfield indicates the selected data rate for the next incoming data frame. The values of two subfields in PLCP headers for RTS and data frames are the same. After a sender sends a RTS frame at the base rate, a receiver estimates the channel and sends back a CTS frame to the sender with the selected rate stored in the *next rate* subfield. The sender modulates the fragment with the rate and sends a data frame to the receiver. After receiving the frame, the receiver predicts the channel condition for the next data frame and sends an ACK frame to the sender with the selected rate.

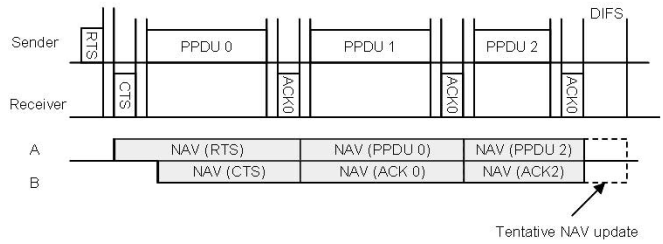

Fig. 5. NAV update process in the proposed protocol.

C. NAV Update

In the proposed dynamic fragmentation scheme, the NAV update process is simpler than that in the RBAR protocol as described in Section II. Fig. 5 explains the NAV update process in the proposed protocol. Because the durations of all fragments in a fragment burst, except for the last fragment, are the same regardless of the data rate, an overhearing node can update the NAV value to the predefined duration when the *More Fragments bit* in the MAC header is set to 1. For the last fragment whose *More Fragments bit* is set to 0, the two-step process for NAV update proposed in the RBAR applies. At first, an overhearing node updates the NAV value with the duration of the normal data frame. This is called a tentative update as shown in Fig. 5. When the last fragment and ACK frame are received, the NAV value is changed to the duration value in the MAC header because the duration values of the MAC headers in the last fragment and the ACK frame indicate the duration of the current transmission.

IV. Performance Evaluation

A. Wireless Channel Model

To reflect the fact that the surrounding environmental clutter may be significantly different for each pair of communication stations with the same distance separation, we use the log-normal shadowing channel model [21]. The path loss $\overline{\mathrm{PL}}$ at distance d is

$$\overline{\mathrm{PL}}(d)\ [\mathrm{dB}] = \overline{\mathrm{PL}}(d_0)\ [\mathrm{dB}] + 10n\log\left(\frac{d}{d_0}\right) + X_\sigma \qquad (3)$$

where d_0 is the close-in reference distance, n is the path loss exponent, and X_σ is a zero-mean Gaussian distributed random variable (in dB) with standard deviation σ (in dB). We set n to 2.56 and σ to 7.67 according to the result of measurements for a wideband microcell model [21]. To estimate $\overline{\mathrm{PL}}(d_0)$, we use the Friis free space equation

$$P_r(d_0) = \frac{P_t G_t G_r \lambda^2}{(4\pi)^2 d_0^2 L} \qquad (4)$$

where P_t and P_r are the transmit and receive power, G_t and G_r are the antenna gains of the transmitter and receiver, λ is the carrier wavelength, and L is the system loss factor, which is set to 1 in our simulation. Most of the simulation parameters are

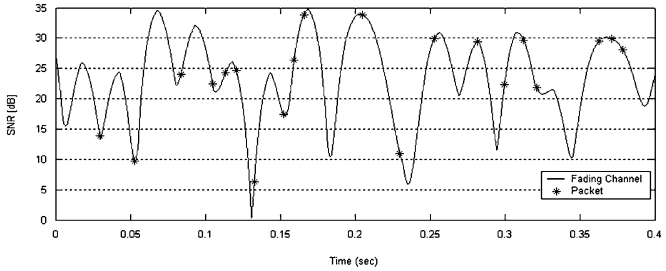

Fig. 6. Packet arrival time on fading channel.

drawn from the data sheet of Cisco 350 client adapter [23] (e.g., the output power, antenna gain).

Finally, the long-term SNR is

$$\mathrm{SNR}_L\ [\mathrm{dB}] = P_t - \overline{\mathrm{PL}}(d) - N + \mathrm{PG}\ [\mathrm{dB}] \tag{5}$$

where N is the noise power, which is set to -95 dBm from [10]. In (5), PG is the spread spectrum processing gain given by

$$\mathrm{PG}\ [\mathrm{dB}] = 10 \cdot \log_{10}\left(\frac{C}{B}\right) \tag{6}$$

where C is the number of chips per symbol and B is the number of bits per symbol. We assume the signal formats in IEEE 802.11b are employed. The numbers of chips per symbol are 11 chips for 1 and 2 Mbps and 8 chips for 5.5 and 11 Mbps. From [26], the PGs for 1, 2, 5.5, and 11 Mbps are 10.4, 7.4, 3, and 0 dB, respectively. For 11 Mbps, because 8 information bits are encoded into an 8-chip sequence, there is no spreading. We evaluate the performance of the proposed scheme in a time-correlated fading channel. The received SNR_L is varied by the Ricean fading gain α, which is generated according to the modified Clack and Gans fading model [20]. The Ricean fading gain α is obtained from a complex Gaussian random variable with mean $\sqrt{K/(K+1)}$ and variance $1/(2(K+1))$, where $K \geq 0$ is the Ricean parameter, defined as the ratio of direct-to-diffuse power in the received signal. Under this model, the SNR of the received signal is

$$\mathrm{SNR}\ [\mathrm{dB}] = 20 \cdot \log_{10}\alpha + \mathrm{SNR}_L\ [\mathrm{dB}]. \tag{7}$$

The time-varying nature of the wireless channel is described by the Doppler spread and coherence time, which are inversely proportional to one another. In our simulations, we consider the effect of the node speed on the change of the Doppler spread and coherence time. All nodes are assumed to move with the same speed. The maximum node speed in our simulation is 7 m/s. Fig. 6 shows the instances of data frame transmissions of one node over the time-correlated Ricean fading channel described previously. In our simulator, a precomputed data set for fading gains is used as suggested in [20]. Each fading gain in the set is applied to (7) for constant time duration defined in [20]. Once a node accesses the channel, the starting point on the data set is randomly chosen. Whenever the constant time duration is passed, the next fading gain from the set is applied to the channel. For the channel condition estimation and prediction in our simulations, we use the SNR measured at the end of the reception of RTS and data frames for the next fragment transmission. In practice, more practical prediction and tracking algorithms are needed (e.g., the adaptive long-range prediction scheme in [24] and [31]). The performance of the proposed scheme in the presence of prediction errors is also evaluated.

TABLE I
SIMULATION PARAMETERS

Parameter	Value
CWmin	31
CWmax	1023
SIFS Time	10 us
DIFS Time	50 us
Slot Time	20 us
MAC Header	272 bits
PHY Header	48 bits
Preamble	144 us
ACK frame length	112 bits
RTS frame length	160 bits
CTS frame length	112 bits

B. Network Setting

We assume all nodes are uniformly distributed in space and within the radio range of each other so the hidden and exposed terminal problems are not considered. The maximum distance between any two nodes is limited to 300 m, which is the maximum effective transmission range as simulated in [12]. For simplicity, we assume the PHY and MAC headers of all types of frames are modulated at the base rate and always reliably received. Because the control frames such as RTS, CTS, and ACK frames are much shorter than data frames, no transmission failure of these frames are considered in the simulation. The parameters used in this simulation studies are shown in Table I. The choice of these parameters is based on the IEEE 802.11b DSSS standards.

To demonstrate the ability of the proposed protocol to adapt to the changing channel condition, we assume the system adapts the data rate by properly choosing one from a set of modulation schemes according to the channel condition. The set of modulation schemes used in this simulation studies are DBPSK, DQPSK, 5.5 complementary code keying (CCK), and 11 CCK as defined in the standard [30]. One of the modulation schemes is chosen so a target PER can be achieved at the current channel SNR level. For simplicity, we refer to the PPDU as a packet in this section commonly used in a physical layer research community.

The base data rate is set to 1 Mbps and the *aFragmentationThreshold* at the base rate is set to 800 octets [25]. Thus, the number of symbols, N, in an MPDU, except for the last one, is set to 6400. However, the symbol rates according to the modulation type are different. The symbol rate for 1 and 2 Mbps is 1 million symbols per second (MSps), and that for 5.5 and 11 Mbps is 1.375 MSps as shown in [26] and [27]. As a consequence, the values of Ns are 6 400 for 1 and 2 Mbps and 8800

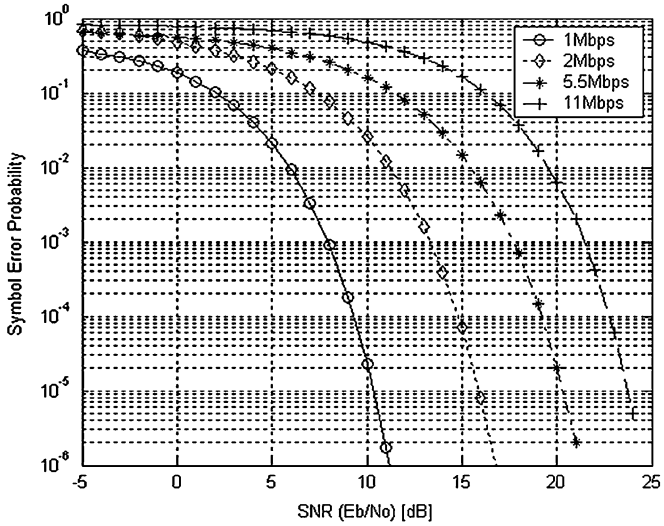

Fig. 7. Symbol error rates of DBPSK, DQPSK, 5.5 CCK, and 11 CCK.

for 5.5 and 11 Mbps. The SER equations for determining the SNR are found over an additive white Gaussian channel in [21]. Because our simulations are performed over the slow-fading channel scenario, the channel slowly changes within a packet. Therefore, we can assume the symbol errors within a packet are approximately independent and use the SERs over the additive white Gaussian channel. For DBPSK,

$$\mathrm{SER} = \frac{1}{2} e^{-E_s/N_0} \tag{8}$$

where E_s/N_0 is the SNR per symbol. The approximated SER for DQPSK found in [29] is given by

$$\mathrm{SER} \leq 2 \cdot Q\left(\sqrt{\frac{E_s}{N_0}}\right). \tag{9}$$

The CCK is a variation of M-ary biorthogonal keying (MBOK) modulation [26], [28]. From [22], the SER is

$$\mathrm{SER} = 1 - \frac{1}{\sqrt{2\pi}} \cdot \int_X^{\infty} \left(\frac{1}{\sqrt{2\pi}} \cdot \int_{-(v+X)}^{v+X} e^{-x^2/2}\, dx \right)^{M/2-1} \cdot e^{-v^2/2}\, dv \tag{10}$$

where $X = \sqrt{(2E_s)/(N_0)}$, and M is 4 for 5.5 Mbps and 8 for 11 Mbps.

Based on the independent symbol error approximation, the PER is related to the SER by

$$\mathrm{PER} = 1 - (1 - \mathrm{SER})^N \tag{11}$$

where N is the number of symbols in a data packet. We set the target PER to 8% according to the IEEE 802.11 standard [8].

By consulting the SER performance curves calculated from (8) to (10) in Fig. 7, the SNR ranges for the corresponding modulation schemes that the target SER is satisfied are, respectively,

$$R = \begin{cases} 1(\mathrm{DBPSK}), & \mathrm{SNR} < \mathrm{SNR}_2 \\ 2(\mathrm{DQPSK}), & \mathrm{SNR}_2 \leq \mathrm{SNR} < \mathrm{SNR}_{5.5} \\ 5.5(\mathrm{CCK}), & \mathrm{SNR}_{5.5} \leq \mathrm{SNR} < \mathrm{SNR}_{11} \\ 11(\mathrm{CCK}), & \mathrm{SNR}_{11} \leq \mathrm{SNR} \end{cases} \tag{12}$$

where SNR_i is the SNR threshold for the data rate i to meet the target SER. The i is replaced by 2 or 5.5 or 11 in equation (12). The SNR ranges for the conventional fragmentation scheme described in Section II are different from those of the proposed dynamic fragmentation scheme. Although the target SERs are the same for all data rates in our fragmentation scheme, the target SERs at different data rates for the conventional fragmentation scheme are different because the number of symbols in a data packet changes for different data rates so different SNR ranges are needed to meet the same target FER requirement. Thus, two sets of SNR ranges are used for the two fragmentation schemes.

According to the IEEE 802.11 standard, the maximum MSDU size is 2304 octets. However, because we consider the case of bulky data traffic where an IP packet can be as large as 64 000 octets, we simulate with a larger maximum MSDU size than the maximum MSDU size in IEEE 802.11. Thus, we assume the MSDU size is uniformly distributed over the range from 2304 octets to 6000 octets at each node. In addition, we assume the MSDUs at any node are always available. In the IEEE 802.11 standard, the value of *dot11MAXTransmitMSDULifetime* is 512 ms for the 2304-maximum MSDU size. Because our simulation uses MSDU sizes larger than 2304 octets, *dot11MAXTransmitMSDULifetime* increase in proportion to the rate of 6000 octets and 2304 octets. Thus, *dot11MAXTransmitMSDULifetime* is set to 1.3 s. The station long retry time (SLRC) is set to 7. All simulations are performed for 300 s simulation time. We compare the performance achieved by three different configurations:

- Case 1: rate-based fragmentation thresholding with the proposed dynamic fragmentation scheme (RFT-DF);
- Case 2: rate-based fragmentation thresholding with the conventional fragmentation scheme (RFT-CF);
- Case 3: single fragmentation threshold with the conventional fragmentation scheme (SFT-CF).

C. Impact of Number of Nodes

Fig. 8 shows the throughputs obtained by these three configurations with Ricean parameter $K = 2$ and 4 m/s node speed as the number of nodes increases from 10 to 130 with step size 30. From Fig. 8, we observe that the throughput of RTF-DF is up to 22% higher than that of SFT-CF and 30.6% higher than that of RTF-CF. Moreover, we observe that increasing the number of nodes from 10 to 130 causes 3.7% degradation in throughput. The idle time caused by one collision is the sum of the backoff time, RTS/CTS transmission time, one SIFS, and one DIFS. This idle time duration is small compared with the lost time caused by data packet errors. In addition, in the fragment burst transmission, the channel access time of a node is longer than that of a single data packet transmission because once the node gains channel access it transmits several fragments without any

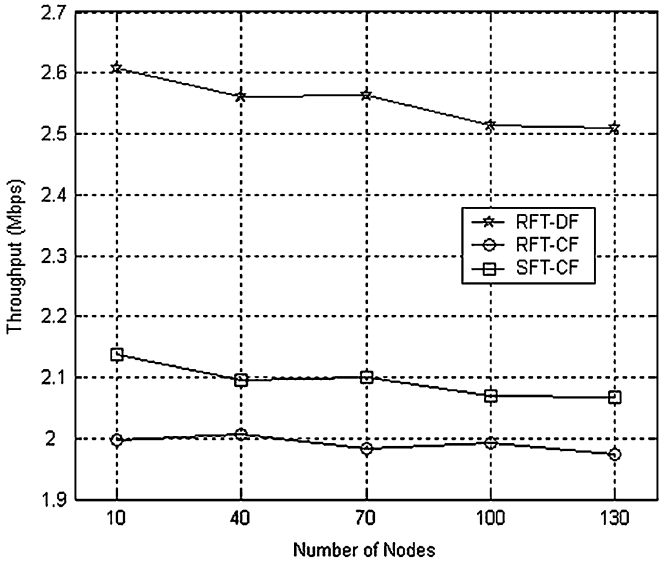

Fig. 8. Throughput as a function of the number of nodes.

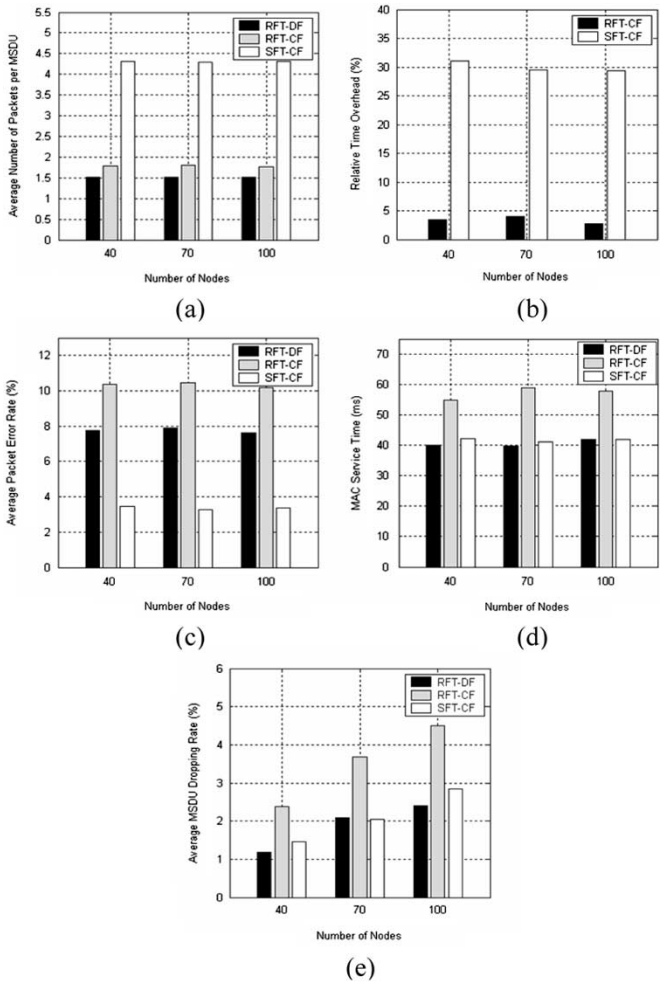

Fig. 9. Performances evaluations as a function of number of nodes for the three schemes: (a) average number of packets per MSDU, (b) relative time overload, (c) average packet error rate, (d) MAC service time, and (e) average MSDU dropping rate.

further contention. Thus, the effect of [Fig. 9(e)] collisions due to the larger number of nodes on the throughput is small. In the simulation, we observe that only 6.7% of the total simulation time in RFT-DF with 130 nodes is caused by contention. A detailed evaluation of the performance differences among three configurations [Figs. 9(a) and (b)] is presented in Fig. 9.

Fig. 9(a) shows the average [Figs. 9(c) and (d)] numbers of packets per MSDU for the three configurations. The number of packets in SFT-CF is about three times of that in RFT-DF. The time overheads relative to RFT-DF are shown in Fig. 9(b). The time overhead relative to RFT-DF is defined as

$$\mathrm{RTO}[\%] = \frac{\mathrm{TO} - \mathrm{TO}_{\mathrm{RFT-DF}}}{\mathrm{TO}_{\mathrm{RFT-DF}}} \cdot 100 \qquad (13)$$

where TO and $\mathrm{TO}_{\mathrm{RFT-DF}}$ are time overheads of the other configuration and RFT-DF, respectively. The time overheads are caused by backoff time, RTS/CTS/ACK frame transmissions, DIFS/SIFS idle times, preamble, and MAC and PHY headers. The time overhead of SFT-CF is much higher, around 32%, than that of RFT-DF. However, the PER of RFT-DF is higher than that of SFT-CF as shown in Fig. 9(c). Although the SNR threshold is chosen to meet the target PER, RFT-DF has higher FER than SFT-CF has because the large packet size in RFT-DF has a higher probability of experiencing channel change within the packet transmission. Fig. 9(d) shows the average MAC service time. We define MAC service time as the time duration for successful transmission of one MSDU (i.e., the time from the MSDU is ready for transmission to the MSDU is acknowledged for a successful transmission). Contrary to time overhead, the MAC service time includes transmission times of packets, elapsed times caused by packet errors, and waiting times caused by transmissions from the other nodes. We notice that although waiting times account for around 80% of the average MAC service time, they do not affect to the calculation of the throughput. The MAC service time of SFT-CF is about 5% higher than that of RFT-DF. Comparing to the result for time overhead, the difference between RFT-DF and SFT-CF is less significant in terms of MAC service time. This is because the elapsed time caused by packet errors in RFT-DF is larger than that of SFT-CF. In addition, because the waiting times account for a large portion of the average MAC service time, the effect of the time overhead difference on the MAC service time reduces. Finally, the average MSDU dropping rates are shown in Fig. 9(e). The factors affecting MSDU dropping are *dot11MAXTransmitMSDULifetime* and SLRC. However, we observe that *dot11MAXTransmitMSDULifetime* is a main factor affecting MSDU dropping. The difference between RFT-DF and SFT-CF in terms of the average MSDU dropping rates is less significant, similar to the difference between the MAC service time. We observe that a dropped MSDU has more packet errors than does a successfully transmitted MSDU. In addition, a transmission failure leads to additional waiting and idle times to access the channel. These times become longer as the number of nodes increases. Thus, the MSDU dropping rates for the three configurations increase significantly with increasing the number of nodes.

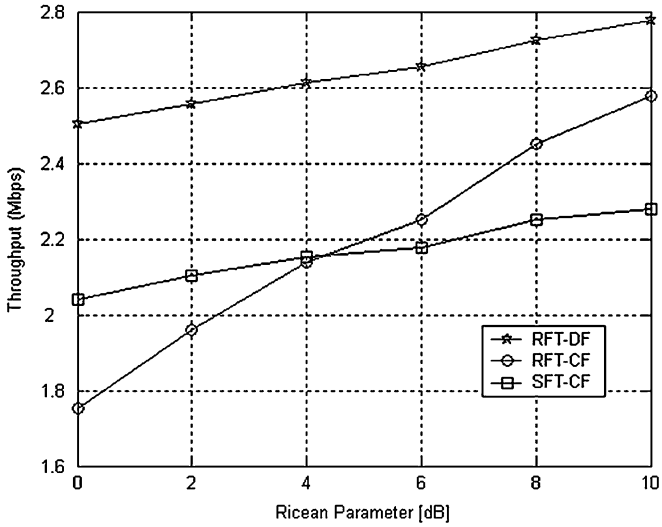

Fig. 10. Throughput as a function of Ricean parameter, K.

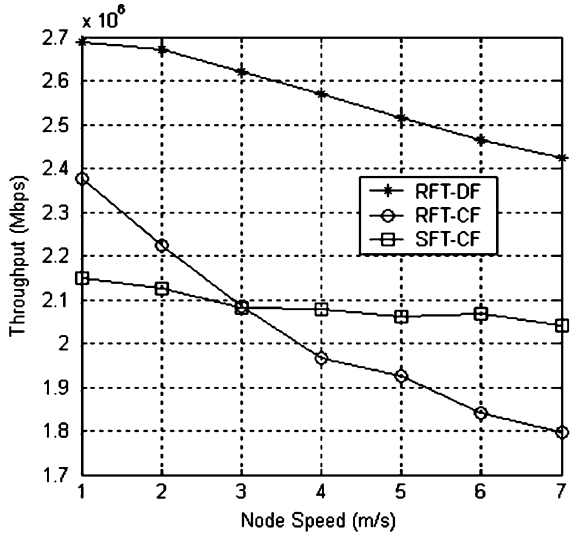

Fig. 11. Throughput as a function of node speed.

D. Impact of Ricean Parameter

Fig. 10 shows the performance of the three configurations described previously under different fading environments with 40 nodes and 4 m/s node speed. The Ricean parameter, K, indicates the strength of the line of the sight component of the received signal. For $K = 0$, the channel has no line-of-sight (LOS) component, corresponding to the worst-case scenario, which is referred to as Rayleigh fading. As K increases, the strength of the LOS component increases. Therefore, the performances of the three configurations improve with increasing K values. From Fig. 10, we observe that the throughput of RFT-DF is up to 21.8% higher than that of SFT-CF at $K = 10$ and 42.8% higher than that of RFT-CF at $K = 0$. For K is bigger than 4, the performance gain of RFT-CF is up to 13.6% higher than that of SFT-CF. As the error rate of the prefragmented MPDUs reduces in the channel with the higher value of K, the gain due to the overhead difference overcomes the loss due to the packet errors.

E. Impact of Node Speed

We vary the speed of nodes but assume that no node is out of the radio range. As the speed of nodes increases, the coherence time of the channel reduces. This implies that the channel changes faster. Fig. 11 shows the performance of the three configurations for seven different speeds ranging from 1 m/s (pedestrian speed) to 7 m/s. The number of nodes is 40, and the Ricean parameter is $K = 2$. From Fig. 11, we observe that the throughput of RFT-DF is 25.2% higher than that of SFT-CF at 1 m/s node speed. The performances of RFT-DF and RFT-CF degrade faster than that of SFT-CF as the node speed increases. This can be explained as follows. As the node speed increases, the channel coherence time is shorter, hence the probability that the channel condition changes in the middle of a packet transmission is higher in the fragmentation scheme with rate-based fragmentation thresholding than in that with a single fragmentation threshold. However, the performance of RFT-DF is still 18.7% higher than that of SFT-CF at 7 m/s node speed. In addition, we notice that when the node speed is less than 3 m/s, the performance of RFT-CF is better than that of SFT-CF. When the nodes move at low speeds, the channel changes slowly enough that it remains constant during one MSDU transmission. At higher speeds, MPDUs fragmented previously in RFT-CF cannot cope with the channel change.

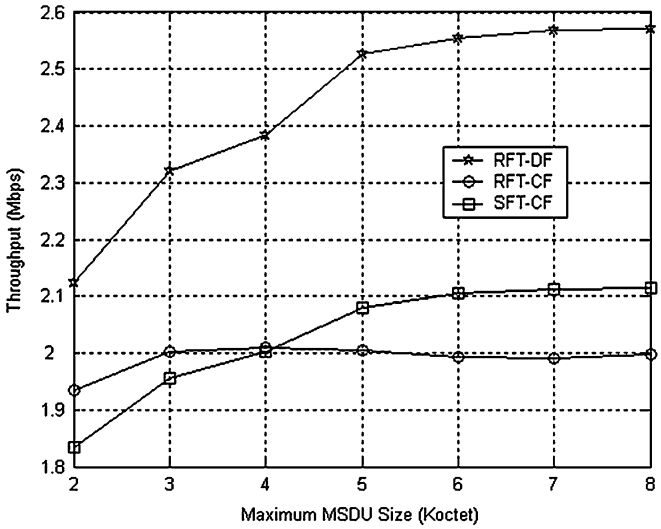

Fig. 12. Throughput as a function of maximum MSDU size.

F. Impact of the Maximum MSDU Size

We also vary the maximum MSDU size from 3000 octets to 10 000 octets with a step size of 1000 octets and observe changes in the performance. According to the maximum MSDU size, *dot11MAXTransmitMSDULifetime* is set to the corresponding value. The number of nodes is 40, the Ricean parameter is $K = 2$, and the node speed is 4 m/s. From Fig. 12, we observe that the throughput of RFT-DF is around 21.6% higher than

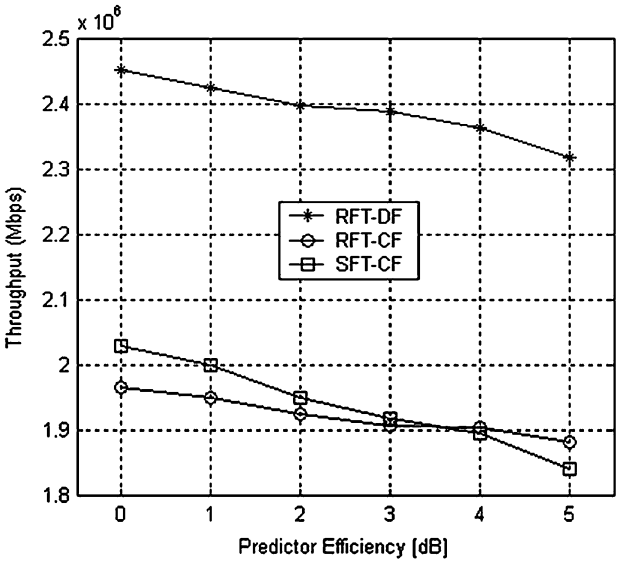

Fig. 13. Throughput as a function of predictor efficiency.

that of SFT-CF. The performance gains of RFT-DF and SFT-CF increase with increasing maximum MSDU size. However, the performance of RFT-CF decreases at large MSDU sizes because the number of prefragmented MPDUs increases with larger MSDU. This makes RFT-CF harder to cope with the channel change.

G. Impact of the Channel Prediction Error

In this section, we evaluate the performance effects by inaccuracy in the channel prediction process. The predicted channel gain, $\widehat{\alpha}$, can be written as

$$\widehat{\alpha} = \alpha + e \tag{14}$$

where α is a true channel gain and e is an additive prediction error, which is assumed to be a white and zero mean complex Gaussian random variable [31], [32]. From studies of the prediction algorithms in [24] and [31]–[33], the prediction error reduces as SNR increases. In this simulation, the channel prediction error variance is defined by

$$\sigma_{\varepsilon}^2\ [\mathrm{dB}] = \gamma\ [\mathrm{dB}] - \mathrm{SNR}\ [\mathrm{dB}] \tag{15}$$

where γ, referred to as *predictor efficiency*, indicates the performance of the channel predictor, namely. In the simulation, we vary the predictor efficiency from 0 to 5 dB. The value of 5 dB corresponds to the worst scenario. The number of nodes is 40, the Ricean parameter is $K = 2$, and the node speed is 4 m/s. From Fig. 13, we observe that the throughput of RTF-DF is up to 25.8% higher than that of SFT-CF and 24.7% higher than that of RTF-CF. Here, even with the inaccurate channel prediction, the proposed scheme still achieves higher performance gain than the other schemes do.

V. Conclusion

In this article, we propose a new rate-adaptive MAC protocol with dynamic fragmentation. The major innovation is the use of multiple fragmentation thresholds for different rates to generate a new fragment from a (remaining) MSDU only after the rate for the next transmission is selected. With this scheme, the nodes with good channels can transmit more data than the ones with bad channel. In addition, the use of constant fragment transmission duration in the physical layer simplifies the process of NAV update in our rate-adaptive system. Our results show that the proposed dynamic fragmentation scheme achieves throughput gain from 14.4% to 29% over the conventional fragmentation scheme used in the IEEE 802.11 MAC protocol.

References

[1] G. O. N. Morinaga, M. Nakagawa, and R. Kohno, "New concepts and technologies for achieving highly reliable and high-capacity multimedia wireless communications systems," *IEEE Commun. Mag.*, pp. 34–40, Jan. 1997.

[2] T. Ikeda, S. Sampei, and N. Morinaga, "TDMA-based adaptive modulation with dynamic channel assignment for high-capacity communication systems," *IEEE Trans. Veh. Technol.*, vol. 49, pp. 404–412, Mar. 2000.

[3] V. K. Lau and Y.-K. Kwok, "On the synergy between adaptive physical layer and multiple-access control for integrated voice and data service in a cellular wireless network," *IEEE Trans. Veh. Technol.*, vol. 51, pp. 1338–1351, Nov. 2002.

[4] J. C.-I. Chuang and N. R. Sollenberger, "Spectrum resource allocation for wireless packet access with application to advanced cellular internet service," *IEEE J. Sel. Area Commun.*, vol. 16, pp. 820–829, Aug. 1998.

[5] S.-T. Sheu, Y.-H. Lee, and M.-H. Chen, "Providing multiple data rate in infrastructure wireless networks," in *Proc. IEEE GLOBECOM'01*, vol. 3, 2001, pp. 1908–1912.

[6] K. K. Leung, P. F. Dricssen, K. Chawla, and X. Qiu, "Link adaptation and power control for streaming service in EGPRS wireless network," *IEEE J. Sel. Area Commun.*, vol. 19, pp. 2029–2039, Oct. 2001.

[7] A. Kramling, M. Siebert, M. Lott, and M. Weckerle, "Interaction of power control and link adaptation for capacity enhancement and QoS assistance," in *Proc. IEEE PIMRC'02*, vol. 2, Sep. 2002, pp. 697–701.

[8] IEEE 802.11 WG, Part II: Wireless LAN Medium Access Control (MAC) and Physical Layer (PHY) specifications, Standard, The IEEE Inc., Piscataway, NJ, 1999.

[9] A. Kamerman and L. Monteban, "WaveLAN-II: A high-performance wireless LAN for the unlicensed band," *Bell Labs. Tech. J.*, pp. 118–133, Summer 1997.

[10] P. Chevillat, J. Jelitto, A. N. Barreto, and H. L. Truong, "A dynamic link adaptation algorithm for IEEE 802.11a wireless LANs," in *Proc. ICC'03*, vol. 2, May 2003, pp. 1141–1145.

[11] G. Holland, N. Vaidya, and P. Bahl, "A rate-adaptive MAC protocol for wireless networks," in *Proc. ACM MOBICOM'01*, Jul. 2001, pp. 236–251.

[12] H.-H. Liu, J.-L. C. Wu, and W.-Y. Chen, "New frame based network allocation vector for 802.11b multirate wireless LANs," in *IEEE Proc. Commun.*, vol. 149, Jun. 2002, pp. 147–151.

[13] B. Sadeghi, V. Kanodia, A. Sabharwal, and E. Knightly, "Opportunistic media access for multirate ad hoc networks," in *Proc. ACM MOBICOM'02*, Sep. 2002, pp. 24–35.

[14] S. Ci and H. Sharif, "A link adaptation scheme for improving throughput in the IEEE 802.11 wireless LAN," in *Proc. IEEE LCN'02*, Nov. 2002, pp. 205–208.

[15] D. Qiao and S. Choi, "Goodput enhancement of IEEE 802.11a wireless LAN via link adaptation," in *Proc. IEEE ICC'01*, vol. 7, Jun. 2001, pp. 1995–2000.

[16] D. Qiao, S. Choi, and K. G. Shin, "Goodput analysis and link adaptation for IEEE 802.11a wireless LANs," *IEEE Trans. Mobile Comput.*, vol. 1, pp. 278–291, Dec. 2002.

[17] J. Tourrihes, "Fragment adaptive reduction: Coping with various interferers in radio unlicensed bands," in *Proc. IEEE ICC'01*, vol. 1, 2001, pp. 239–244.

[18] S. Ci and H. Sharif, "Adaptive approaches to enhance throughput of IEEE 802.11 wireless LAN with bursty channel," in *Proc. IEEE LCN'00*, Nov. 2000, pp. 44–45.
[19] J. Tourrihes, "Dwell adaptive fragmentation: How to cope with short dwells required by multimedia wireless LANs," in *Proc. IEEE GLOBECOM'00*, vol. 1, 2000, pp. 57–61.
[20] R. J. Punnoose, P. V. Nikitin, and D. D. Stancil, "Efficient simulation of Ricean fading within a packet simulator," in *Proc. IEEE VTC'00*, 2000, pp. 764–767.
[21] T. S. Rappaport, "Mobile radio propagation: Large-scale path loss," in *Wireless Communications: Principles and Practices*. Upper Saddle River, NJ: Prentice-Hall, 1996, pp. 69–185.
[22] J. G. Proakis, "Performance of the optimum receiver for memoryless modulation," in *Digital Communications*, 3rd ed., New York, NY: McGraw-Hill, 1995, pp. 257–282.
[23] Cisco Aironet 350 Series Access Points Data Sheet [Online]. Available: http://www.cisco.com/en/US/products/hw/wireless/ps458/products_data_sheet09186a008009247c.html, 2002.
[24] A. Duel-Hallen, S. Hu, and H. Hallen, "Long-range prediction of fading signals," *IEEE Signal Process. Mag.*, pp. 62–75, May 2000.
[25] B. P. Crow, I. Widjaja, J. G. Kim, and P. T. Sakai, "IEEE 802.11 wireless local area networks," *IEEE Commun. Mag.*, pp. 116–126, Sep. 1997.
[26] M. Fainberg "A Performance Analysis of the IEEE 802.11b Local Area Network in the Presence of Bluetooth Personal Area Network", M.S. Thesis, Electrical Comput. Eng. Dept., Polytechnic University, Brooklyn, NY, Jun. 2001.
[27] B. Pearson, "Complementary Code Keying Made Simple," Intersil, Milpitas, CA, USA, Application Notes AN9850.1, May 2000.
[28] J. Figueroa, B. Garon, B. Pearson, and A. Petrick, "Technology economics of standards based WLAN solutions and cost of ownership," in *Proc. WTC'99*, China, 1999, pp. 70–74.
[29] J. G. Proakis and M. Salehi, "Differential phase modulation and demodulation," in *Contemporary Communication Systems Using Matlab*. Piscataway, NJ: Brooks/Cole Thomson Learning, 2000, pp. 302–309.
[30] Supplement to IEEE Standard for Information Technology—Telecommunications and Information Exchange Between Systems—Local and Metropolitan Area Networks—Specific Requirements Part 11: Wireless LAN Medium Access Control (MAC) and Physical Layer (PHY) Specifications: Higher-Speed Physical Layer Extension in the 2.4 GHz Band, Standard., Piscataway, NJ, Sep., 1999.
[31] S. Falahati, A. Svensson, M. Sternad, and T. Ekman, "Adaptive modulation system for predicted wireless channels," in *Proc. IEEE GLOBECOM'03*, vol. 1, 2003, pp. 357–361.
[32] A. Aguiar, H. Karl, and A. Wolisz, "Channel adaptive techniques in the presence of channel prediction inaccuracy," presented at the European Wireless Conference 2004, Barcelona, Spain, Feb. 2004.
[33] T. Ekman "Prediction of Mobile Radio Channels, Modeling and Design", Ph.D. thesis, Uppsala Univ., Uppsala, Sweden, Oct. 2002.

Byung-Seo Kim (S'03) received the B.S. degree in electrical engineering from In-Ha University, In-Chon, Korea, in 1998, and received the M.S. and Ph.D. degrees in electrical and computer engineering from University of Florida, Gainesville, in 2001 and 2004, respectively. Between 1997 and 1999, he worked for Motorola Korea Ltd., PaJu, Korea, as a Computer Integrated Manufacturing Engineer in Advanced Technology Research & Development. Since January 2005, he has been with Motorola, Inc., Schaumburg, IL, where he is currently a Senior Software Engineer in Government & Enterprise Mobility Solutions. His research interests include designing and developing efficient link-adaptable MAC protocol, cross-layer architecture, multi-MAC structure, and resource allocation algorithm for wireless networks.

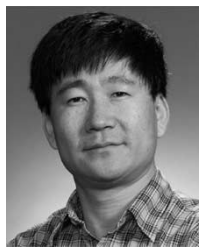

Yuguang (Michael) Fang (S'92–M'94–S'96–M'97–SM'99) received the Ph.D. degree in systems and control engineering from Case Western Reserve University, Cleveland, OH, in January 1994, and the Ph.D. degree in electrical engineering from Boston University, Boston, MA, in May 1997.

From September 1989 to December 1993, he was a Teaching/Research Assistant in the Department of Systems, Control and Industrial Engineering, Case Western Reserve University, where he held a Research Associate position from January 1994 to May 1994. He held a postdoctoral position in the Department of Electrical and Computer Engineering, Boston University, from June 1994 to August 1995. From September 1995 to May 1997, he was a Research Assistant in the Department of Electrical and Computer Engineering, Boston University. From June 1997 to July 1998, he was a Visiting Assistant Professor in Department of Electrical Engineering, University of Texas at Dallas. From July 1998 to May 2000, he was an Assistant Professor in the Department of Electrical and Computer Engineering, New Jersey Institute of Technology, Newark. In May 2000, he joined the Department of Electrical and Computer Engineering, University of Florida, Gainesville, where he got an early promotion with tenure in August 2003 and has since then been an Associate Professor. His research interests span many areas, including wireless networks, mobile computing, mobile communications, automatic control, and neural networks. He has published more than 140 papers in refereed professional journals and conferences.

Dr. Fang has actively engaged in many professional activities. He is a member of the ACM. He is an Editor for *IEEE Trans. Commun.*, an Editor for *IEEE Trans. Wireless Commun.*, an Editor for *IEEE Trans. Mobile Comput.*, a Technical Editor for *IEEE Wireless Commun. Mag.*, an Editor for *ACM Wireless Networks*, and an Area Editor for *ACM Mobile Comput. Commun. Rev.* He was an Editor for *IEEE J. Select. Area Commun.: Wireless Communications Series* from May 1999 to December 2001, an Editor for *Wiley International Journal on Wireless Communications and Mobile Computing* from April 2000 to January 2004, and the Feature Editor for Scanning the Literature in *IEEE Pers. Commun.* (now *IEEE Wireless Commun.*) from April 2000 to April 2003. He is also actively involved with many professional conferences. He is the General Chair for the Second International Conference on Quality of Service in Wired/Wireless Networks (QShine'2005) and the Technical Program Vice-Chair for IEEE INFOCOM'2005. He was the Program Co-Chair for the Global Internet and Next Generation Networks Symposium in IEEE Globecom'2004 and the Program Vice Chair for 2000 IEEE Wireless Communications and Networking Conference (WCNC'2000), where he received the IEEE Appreciation Award for service to this conference. He has served on many Technical Program Committees such as IEEE INFOCOM (2005, 2004, 2003, 2000, and 1998), IEEE ICC (2004), IEEE Globecom (2004, 2003, and 2002), IEEE WCNC (2004, 2002, 2000, and 1999), and ACM MobiCom (2001). He served as the Committee Co-Chair for Student Travel Award for 2002 ACM MobiCom. He was the Vice-Chair for the IEEE Gainesville Section in 2002 and 2003, and is the Chair in 2004 and 2005. He received the National Science Foundation Faculty Early Career Award in 2001 and the Office of Naval Research Young Investigator Award in 2002.

Tan F. Wong (M'98–SM'03) received the B.S. degree (first-class honors) in electronic engineering from the Chinese University of Hong Kong, Hong Kong, China, in 1991, and the M.S.E.E. and Ph.D. degrees in electrical engineering from Purdue University, West Lafayette, IN, in 1992 and 1997, respectively.

He was a Research Engineer working on the high-speed wireless networks project in the Department of Electronics, Macquarie University, Sydney, Australia. He also served as a postdoctoral Research Associate in the School of Electrical and Computer Engineering, Purdue University. Since August 1998, he has been with the University of Florida, Gainesville, where he is currently an Associate Professor of electrical and computer engineering. He serves as Editor for Wideband and Multiple Access Wireless Systems for the *IEEE Trans. Commun.* and as Editor for the *IEEE Trans. Veh. Technol.*

Younggoo Kwon received the B.S. and M.S. degrees in electrical engineering from Korea University, Seoul, Korea, in 1993 and 1996, respectively, and the Ph.D. degree in electrical engineering from the Department of Electrical and Computer Engineering, University of Florida, Gainesville, in 2002.

From 2002 to 2003, he was a Senior Member of the Research Staff at Samsung Electro-Mechanics Central R&D Center, Suwon, Korea. Since 2004, he has been an Assistant Professor in the Department of Computer Engineering, Sejong University, Seoul, Korea. He has authored/co-authored more than ten technical papers and book chapters in the areas of wireless/mobile networks and RFID/Ubiquitous Sensor Networks. His current research interests include the area of RFID/USN systems with emphasis on the energy-efficient network protocols, and the quality-of-service guarantee and adaptation in MAC layer for multimedia home networking based on wireless LANs and wireless PANs.